

Brownian Dynamics in Fourier Space: Membrane Simulations over Long Length and Time Scales

Lawrence C.-L. Lin¹ and Frank L. H. Brown²

¹*Department of Physics, University of California, Santa Barbara, California 93106-9530, USA*

²*Department of Chemistry and Biochemistry, University of California, Santa Barbara, California 93106-9510, USA*

(Received 7 July 2004; published 14 December 2004)

A simulation algorithm for elastic membrane sheets is presented. Overdamped stochastic dynamics including hydrodynamic coupling to surrounding solvent and arbitrary external forces are generated by employing Fourier modes of the sheet as the primary dynamic variables. Simulations over the micron length scale and second time scale are easily achieved. The dynamics of a lipid bilayer attached to an underlying network of cytoskeletal filaments is used to estimate the diffusion constant of membrane-bound proteins on the surface of the red blood cell.

DOI: 10.1103/PhysRevLett.93.256001

PACS numbers: 83.10.Mj, 87.15.Vv, 87.16.Ac, 87.16.Dg

Many interesting phenomena in cellular biology and membrane biophysics involve size and time regimes inaccessible to fully atomic simulations. Simplified models represent our only hope to study such systems theoretically. Analytical progress has been made for studying the dynamics of continuous elastic membranes, but only for interactions that are harmonic in nature within relatively simple geometries [1–3]. Dynamic simulations involving more elaborate harmonic models have been pursued [4], but neglect hydrodynamic effects and thermal fluctuations. Monte Carlo simulations have also successfully treated general nonharmonic potentials [5,6], but yield only time-independent information. In this Letter, we present an efficient membrane simulation technique that accounts for both hydrodynamics and thermal fluctuations in the presence of arbitrary potentials. To our knowledge, this method is the first with such capabilities. Using the techniques developed, we model bilayer fluctuations on the surface of the red blood cell at the micron scale over seconds in time. The algorithm we present provides a potential means for simulating a large class of problems in membrane biophysics.

Our starting point is the elastic energy for a tensionless fluid quasiplanar sheet [7,8] with external perturbations

$$H = \int_{\mathcal{A}} d\mathbf{r} \left\{ \frac{K_c}{2} [\nabla^2 h(\mathbf{r})]^2 + \mathcal{H}_{\text{int}}[h(\mathbf{r})] \right\}, \quad (1)$$

where K_c is the bending modulus, $\mathcal{A} = \mathcal{L}^2$ is the projected membrane area, $\mathbf{r} = (x, y)$ is the position in the xy plane, and $h(\mathbf{r})$ specifies the height of the membrane above the reference plane at $h(\mathbf{r}) = 0$. The interaction term $\mathcal{H}_{\text{int}}[h(\mathbf{r})]$ allows for arbitrary interactions between the membrane and its surroundings. Although we consider tensionless systems here, the equations are easily generalizable by adding a surface tension term. Equation (1) is expected to hold down to wavelengths of $\sim 3\text{--}6$ nm [9]. Finer resolution would require a more microscopic approach.

Stochastic dynamics appropriate to the low Reynolds number regime and small out-of-plane fluctuations are

described by a nonlocal Langevin equation in an infinitely periodic geometry (period \mathcal{L} in x and y) [10]

$$\frac{\partial h(\mathbf{r}, t)}{\partial t} = \int_{-\infty}^{\infty} d\mathbf{r}' \Lambda(\mathbf{r} - \mathbf{r}') [F(\mathbf{r}', t) + \zeta(\mathbf{r}', t)], \quad (2)$$

where $\Lambda(\mathbf{r} - \mathbf{r}') = 1/8\pi\eta|\mathbf{r} - \mathbf{r}'|$ is the diagonal portion of the Oseen tensor, η is the viscosity of the surrounding fluid, $F(\mathbf{r}, t) = -\delta H/\delta h(\mathbf{r}, t)$ and $\zeta(\mathbf{r}, t)$ is a Gaussian white noise satisfying the fluctuation-dissipation relation [11]. These equations completely specify dynamics for the lipid bilayer.

Simple harmonic forms for $\mathcal{H}_{\text{int}}[h(\mathbf{r})]$ in Eq. (1) lead to models that may be pursued analytically [1,2], while complex harmonic interactions require numerics to identify the normal modes [3]. In either case, exact dynamics are attainable for arbitrary time steps. In the case of more general potentials, numerical simulation over sufficiently small time steps provides the only viable means to study the dynamics described above. Introduction of a general dynamics algorithm is the focus of this letter. To begin, we note that the convolution over the nonlocal hydrodynamic interaction is most efficiently handled in Fourier space

$$\frac{\partial h_{\mathbf{k}}(t)}{\partial t} = \Lambda_{\mathbf{k}} \{F_{\mathbf{k}}[h(\mathbf{r}, t)] + \zeta_{\mathbf{k}}(t)\}, \quad (3)$$

where the Fourier transforms are defined by $h_{\mathbf{k}} = \int_{\mathcal{A}} d\mathbf{r} h(\mathbf{r}) e^{-i\mathbf{k}\cdot\mathbf{r}}$ and $h(\mathbf{r}) = \mathcal{L}^{-2} \sum_{\mathbf{k}} h_{\mathbf{k}} e^{i\mathbf{k}\cdot\mathbf{r}}$, $\Lambda_{\mathbf{k}} = 1/4\eta k$, and $\zeta_{\mathbf{k}}(t)$ now obeys $\langle \zeta_{\mathbf{k}}(t) \rangle = 0$ and $\langle \zeta_{\mathbf{k}}(t) \zeta_{\mathbf{k}'}(t') \rangle = 2k_{\text{B}} T \mathcal{L}^2 \Lambda_{\mathbf{k}}^{-1} \delta_{\mathbf{k}, -\mathbf{k}'} \delta(t - t')$. For general potentials, $F_{\mathbf{k}}$ is a functional of the height field of the membrane and is dependent upon the entire set of amplitudes $h_{\mathbf{k}}$; Eq. (3) describes a set of coupled equations. Wave vectors are limited to values commensurate with the periodicity of the system so that $\mathbf{k} = (m, n)2\pi/\mathcal{L}$ and a short wavelength cutoff is imposed to confine $-N/2 < m, n \leq N/2$, corresponding to discretization in the (x, y) plane by $\ell = \mathcal{L}/N$.

The divergence of $\Lambda_{\mathbf{k}=0}$ is a nonphysical consequence of our periodic boundary conditions. The problem becomes

irrelevant in systems where it is appropriate to fix the center of mass so that it cannot move ($\Lambda_0 = 0$). For systems where we require center of mass motion, we take $\Lambda_0 \approx 3\mathcal{L}/8\pi\eta$ reflecting diffusion of a membrane patch of area \mathcal{A} [3]. Although we use this value in several of our simulations, it was verified that none of the results depend on this choice.

A simulation algorithm based on Eq. (3) follows from the principles of Brownian dynamics [12] with slight modifications. The equations of motion are integrated from t to $t + \Delta t$ for small Δt

$$h_{\mathbf{k}}(t + \Delta t) = h_{\mathbf{k}}(t) + \Lambda_{\mathbf{k}} F_{\mathbf{k}}(t) \Delta t + R_{\mathbf{k}}(\Delta t), \quad (4)$$

$$R_{\mathbf{k}}(\Delta t) \equiv \Lambda_{\mathbf{k}} \int_t^{t+\Delta t} dt' \zeta_{\mathbf{k}}(t'),$$

and the real and imaginary components of $R_{\mathbf{k}}(\Delta t)$ are drawn from Gaussian distributions of appropriate width. However, the Fourier modes obey the relation $h_{\mathbf{k}}^* = h_{-\mathbf{k}}$ since $h(\mathbf{r})$ is a real quantity. As a result, the real and imaginary parts of the amplitudes $h_{\mathbf{k}}$ are not completely independent and only half of the equations implied by Eq. (4) are evolved in time. The modes given by $(m, n) = (0, 0)$, $(N/2, 0)$, $(0, N/2)$, and $(N/2, N/2)$ are completely real and comprise four independent dynamic variables for the system. We choose the other independent modes to be (m, n) for $-N/2 < m < N/2$ and $0 < n < N/2$, $(m, 0)$ for $0 < m < N/2$, $(m, N/2)$ for $0 < m < N/2$, and $(N/2, n)$ for $0 < n < N/2$. The real and imaginary parts of each of these modes comprise additional independent dynamic variables. The remaining modes are related by complex conjugation to these independent modes.

The considerations above also apply to the random force $\zeta_{\mathbf{k}} \equiv f_{\mathbf{k}} + ig_{\mathbf{k}}$. The fluctuation-dissipation relation for the purely real components is $\langle f_{\mathbf{k}}(t) f_{\mathbf{k}}(t) \rangle = 2k_B T \mathcal{L}^2 \Lambda_{\mathbf{k}}^{-1} \delta(t - t')$ while the remaining independent components exhibit $\langle f_{\mathbf{k}}(t) f_{\mathbf{k}}(t) \rangle = \langle g_{\mathbf{k}}(t) g_{\mathbf{k}}(t) \rangle = k_B T \mathcal{L}^2 \Lambda_{\mathbf{k}}^{-1} \delta(t - t')$. Cross correlations between the amplitudes $f_{\mathbf{k}}$ and $g_{\mathbf{k}}$ are all zero. Correspondingly, $R_{\mathbf{k}}(\Delta t)$ is drawn from a Gaussian distribution with zero mean and variance $2\mathcal{L}^2 k_B T \Lambda_{\mathbf{k}} \Delta t$ for the explicitly real modes and the real and imaginary parts of $R_{\mathbf{k}}(\Delta t)$ are drawn from a Gaussian distribution with zero mean and variance $\mathcal{L}^2 k_B T \Lambda_{\mathbf{k}} \Delta t$ for the remaining independent modes.

Simulations proceed from some initial configuration for the sheet [typically $h(\mathbf{r}) = 0$] and evolve forward in time on the basis of Eq. (4). Explicitly, a single time step in the simulation algorithm consists of four parts: (1) Evaluate the interaction part of the forces $F_{\text{int}}(\mathbf{r}) = -\delta H_{\text{int}}/\delta h(\mathbf{r})$ in position space. (2) Compute the bending forces $F_{\mathbf{k}}^{\text{bend}} = -K_c k^4 h_{\mathbf{k}}$ and evaluate the interaction force $F_{\mathbf{k}}^{\text{int}}$ by Fourier transforming the result of the previous step. (3) Draw $R_{\mathbf{k}}(\Delta t)$'s from the appropriate Gaussian distributions. (4) Compute $h_{\mathbf{k}}(t + \Delta t)$ using Eq. (4). Inverse Fourier transformation yields $h(\mathbf{r})$ for use in the next iteration. Of

course, Δt must be chosen small enough to ensure convergence. From this point forward, we refer to this algorithm as Fourier space Brownian dynamics (FSBD) [13].

We demonstrate the stability of FSBD by comparing with known results for systems whose equations of motion can be solved analytically. The simplest case is that of the free membrane for which $\mathcal{H}_{\text{int}} = 0$. The exact result for the height correlation function is [10]

$$\frac{\langle h(t)h(0) \rangle}{\langle h^2 \rangle} = \frac{\sum_{\mathbf{k}} k^{-4} e^{-\omega_{\mathbf{k}} t}}{\sum_{\mathbf{k}} k^{-4}}, \quad (5)$$

where the relaxation frequencies are $\omega_{\mathbf{k}} = K_c k^3/4\eta$. A comparison between simulation and exact results is shown in Fig. 1.

A more interesting case for which results can be obtained semianalytically is that of a membrane harmonically pinned by a localized potential

$$\mathcal{H}_{\text{pin}}[h(\mathbf{r})] = \frac{\gamma}{2} h^2(\mathbf{r}) \sum_i \exp\left[-\left(\frac{\mathbf{r} - \mathbf{R}_i}{\ell/4}\right)^2\right], \quad (6)$$

where $\ell = \mathcal{L}/N$ and γ is sufficiently large that the height is essentially zero near the pinning sites \mathbf{R}_i labeled by the index i . We study the case where the membrane is pinned at a single site $\mathbf{R} = 0$ (and therefore all four corners by the periodic boundary conditions). Exact results for the auto-correlation function, taken from Ref. [3], are compared to FSBD simulation in Fig. 1.

As a validation of FSBD outside the harmonic regime, we compare equilibrium properties for a membrane confined between two walls located at $\pm a$ to Monte Carlo data

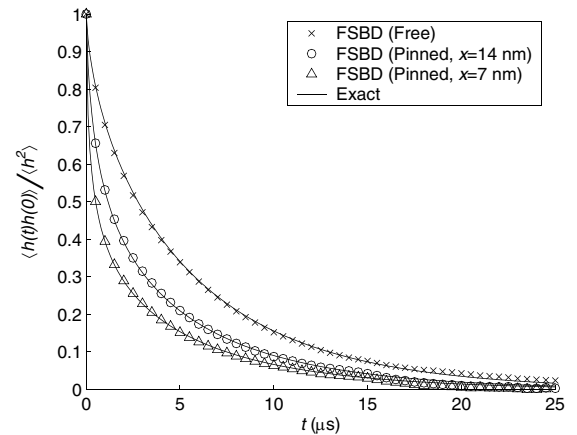


FIG. 1. Plot of the normalized height autocorrelation function for a free membrane and a membrane pinned at the corners of a square $\mathcal{L} = 112$ nm, $\ell = 7$ nm, and $N = 16$. All plots are for $y = 0$, $\Delta t = 1$ ns, $\Lambda_0 = 0$, and a total simulation time of $t = 0.1$ s. The values used for the physical parameters are $K_c = 2 \times 10^{-13}$ ergs, $\eta = 0.06$ P, and $T = 310$ K, and the value of the pinning constant for the pinned system is $\gamma = 2 \times 10^{14}$ ergs cm $^{-4}$. The magnitude of deviation from the exact answers is consistent with standard statistical error estimates [23].

previously reported for the same system [5]. The form of the interaction potential, intended to mimic that of a stack of membranes, is

$$\mathcal{H}_{\text{wall}}[h(\mathbf{r})] = \frac{1}{2}\{V[a + h(\mathbf{r})] + V[a - h(\mathbf{r})]\}, \quad (7)$$

where $V(z) = A\lambda \exp(-z/\lambda) - H/12\pi z^2$, and A , H , and λ are constants. The quantities computed by Gouliarov and Nagle [5] are the root mean square displacement $\sigma \equiv \sqrt{\langle h^2 \rangle}$ and the pressure P that the membrane exerts on the walls. A comparison between Monte Carlo and FSBD results are reported in Table I. Within statistical error, the results of the two methods are identical.

We now focus on a biophysical problem requiring anharmonic dynamic membrane simulations over long length and time scales. The mobility of band 3 protein on the red blood cell surface has been closely scrutinized [14,15] and is known to be influenced by interactions between band 3 and the spectrin cytoskeletal network attached to the membrane surface [14]. The spectrin network forms a series of ~ 100 nm diameter corrals on the cell surface which hinder the diffusive behavior of proteins [14,15]. On short length scales $D \approx 0.53 \mu\text{m}^2 \text{s}^{-1}$ [15], reflecting unhindered diffusion within a single corral. The protein protrudes a distance, h_0 , into the cell and this intracellular domain clashes with cytoskeletal filaments leading to a large decrease in diffusivity $D_{\text{macro}} \approx 6.6 \times 10^{-3} \mu\text{m}^2 \text{s}^{-1}$ [15] over cellular length scales. Given the strong confining influence of the cytoskeleton, it is somewhat remarkable that band 3 does manage to explore the entire cell surface. The exact mechanism leading to corral hopping events remains poorly understood.

Many previous studies have focused on dynamic rearrangements of the cytoskeleton as a possible mechanism leading to band 3 escape from individual corrals [14–18]. Recently, we suggested thermal fluctuations of the bilayer itself as a potential means to promote corral hopping events [3]. Here we again focus our attention on bilayer fluctuations (we assume the cytoskeleton is static), but improve upon previous work by including a more realistic interac-

tion between the cytoskeleton and the membrane. The bilayer is both pinned to the cytoskeleton at discrete points and repelled by the filaments between pinning sites. FSBD makes such a simulation possible whereas the harmonic dynamics scheme introduced previously [3] is unable to account for filament-membrane repulsion.

We approximate repulsive interactions between the membrane and spectrin cytoskeleton as a short-range hydration interaction of the form [19]

$$\mathcal{H}_{\text{rep}} = \epsilon \sum_i e^{-h(\mathbf{r})/\lambda} \exp\left[-\left(\frac{a_i x + b_i y + c_i}{\ell/4}\right)^2\right], \quad (8)$$

where $a_i x + b_i y + c_i = 0$ specifies a particular finite linear segment of spectrin between pinning sites. Pinning of the membrane to spectrin at the ends of these segments is accomplished via harmonic interactions as in Eq. (6). We choose $\lambda = 0.2$ nm [20], $\epsilon = k_B T/100\ell^2$, and $\gamma = 2 \times 10^{14}$ ergs cm^{-4} , ensuring strong pinning (increasing γ does not affect results) and a steeply rising hydration potential that effectively prevents $h(\mathbf{r}) < 0$ above spectrin filaments. The values for the physical parameters of the red blood cell are $K_c = 2 \times 10^{-13}$ ergs, $\eta = 0.06$ P, $h_0 = 6$ nm, $T = 310$ K, $\ell = 7$ nm and $L = 112$ nm (see Ref. [3], and references therein). Figure 2 displays the geometry of our simulations. Multiple $L \times L$ corrals are simulated within a larger periodic box of edge size \mathcal{L} . For system sizes $\mathcal{L} \geq 4L$ we find no dependence of reported results on Λ_0 and all results are reported in this converged limit.

Our model of protein diffusion closely follows that described in Ref. [3]; readers are directed there for a full discussion. We treat the height of membrane at the corral periphery as a dynamic gating mechanism. The height of the membrane must exceed h_0 for long enough to allow diffusion over the spectrin barrier. Within this picture we find that the addition of repulsive interactions between the cytoskeleton and membrane translates into a twofold lowering of the calculated diffusion constant $D_{\text{macro}} = (3.44 \pm 0.11) \times 10^{-2} \mu\text{m}^2 \text{s}^{-1}$ relative to the value obtained in the absence of repulsive interactions ($D_{\text{macro}} = 7.0 \times 10^{-2} \mu\text{m}^2 \text{s}^{-1}$ [3]). In the more realistic triangular ge-

TABLE I. Comparison of Monte Carlo data [5] with those from FSBD for a membrane confined between two walls. See the text for details and definitions. A time step of $\Delta t = 0.05$ ns was used and the total time of each simulation was $t = 10$ ms. The results for FSBD reflect averaging over significantly more independent samples than the results for Monte Carlo.

N	$\mathcal{L}(\text{\AA})$	$\sigma(\text{\AA})$ (MC)	$\sigma(\text{\AA})$ (FSBD)	$P(\text{ergs}/\text{cm}^3)$ (MC)	$P(\text{ergs}/\text{cm}^3)$ (FSBD)
$A = 10^9 \text{ ergs}/\text{cm}^3, H = 0, K_c = 10^{-12} \text{ ergs}, \lambda = 1.8 \text{ \AA}, T = 323 \text{ K}, a = 20 \text{ \AA}$					
4	700	4.0774 ± 0.0018	4.07689 ± 0.00099	123010 ± 170	122950 ± 80
8	700	4.3366 ± 0.0013	4.33609 ± 0.00063	173470 ± 170	173530 ± 80
16	700	4.3792 ± 0.0034	4.38107 ± 0.00054	193800 ± 600	194130 ± 80
$A = 10^9 \text{ ergs}/\text{cm}^3, H = 3 \times 10^{-14} \text{ ergs}, K_c = 10^{-13} \text{ ergs}, \lambda = 1.4 \text{ \AA}, T = 323 \text{ K}, a = 17 \text{ \AA}$					
4	350	6.0902 ± 0.0027	6.08605 ± 0.00108	28000 ± 900	26700 ± 310
8	700	6.1225 ± 0.0030	6.11984 ± 0.00053	38500 ± 1000	37550 ± 150
16	1400	6.1270 ± 0.0026	6.12994 ± 0.00027	40000 ± 600	40930 ± 80

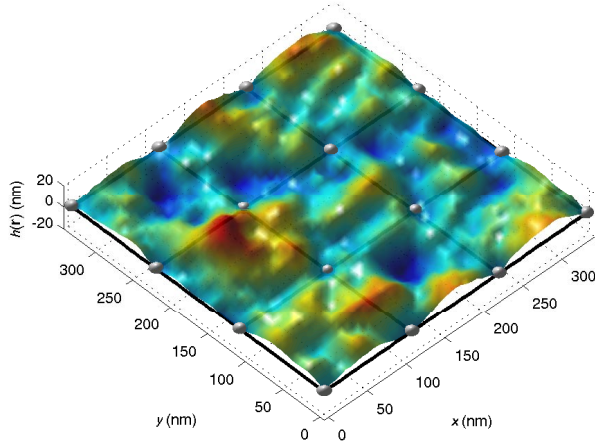


FIG. 2 (color online). Snapshot of a red blood cell membrane evolved with FSBD for $\mathcal{L} = 3L$ using the physical parameters in the text. The spheres indicate where the membrane is pinned to spectrin filaments (represented as dark lines). At the edges of the corrals, the membrane must lie above the plane due to repulsive interaction with the cytoskeleton. The z axis is expanded to emphasize membrane undulations.

ometry of Ref. [3] we find $D_{\text{macro}} = (2.06 \pm 0.13) \times 10^{-2} \mu\text{m}^2 \text{s}^{-1}$ ($D_{\text{macro}} = 6.6 \times 10^{-2} \mu\text{m}^2 \text{s}^{-1}$ with repulsions off [3]), approximately 3 times larger than observed experimentally.

The addition of repulsive interactions decreases the macroscopic diffusion constant by a geometry dependent factor (1/2 for squares, 1/3 for triangles). This is unexpected since repulsions push the membrane above the cytoskeleton and increase the prevalence of h_0 sized gaps. However, the regular network of repulsive filaments effectively quenches modes of wavelength $\sim 2L$ that are present in the absence of repulsion. The remaining modes fluctuate faster than those at longer wavelength; the gaps that do open are apt to close more quickly in the presence of repulsions. This effect accounts for the lowered diffusion constants. Our results indicate that membrane undulations are likely to contribute to the observed diffusion on the surface of the red blood cell. We have voiced this conclusion previously [3], however, the realism of the model enabled by the FSBD approach makes the present study more convincing and the mechanism has been substantially altered. Our study has focused entirely on bilayer fluctuations with complete neglect of cytoskeletal motion. In light of this and the experimental uncertainty present in physical parameters we have adopted, the D_{macro} values we calculate are not expected to be quantitatively correct. Rather, the qualitative implication that membrane undulations should play a role in the diffusive process is the conclusion of this study.

Many processes in biology and membrane biophysics are completely inaccessible to atomistic simulations and the general mesoscopic approach afforded by FSBD should prove invaluable in a number of areas. Problems of cytoskeletal growth at membrane surfaces [21] and the fluctuations observed in “active” membranes [22] and membrane stacks [5] represent just a few examples of problems potentially amenable to such an approach. Future applications for FSBD extend far beyond the single example pursued here.

We thank Professor J.F. Nagle for helpful discussions. This work is supported by the NSF (CHE-0349196).

-
- [1] R. Granek and J. Klafter, *Europhys. Lett.* **56**, 15 (2001).
 - [2] N. Gov, A. G. Zilman, and S. Safran, *Phys. Rev. Lett.* **90**, 228101 (2003); N. Gov and S. A. Safran, *Phys. Rev. E* **69**, 011101 (2004).
 - [3] F. L. H. Brown, *Biophys. J.* **84**, 842 (2003); L. C.-L. Lin and F. L. H. Brown, *ibid.* **86**, 764 (2004).
 - [4] S. Y. Qi, J. T. Groves, and A. K. Chakraborty, *Proc. Nat. Acad. Sci. U.S.A.* **98**, 6548 (2001).
 - [5] N. Gouliarov and J. F. Nagle, *Phys. Rev. E* **58**, 881 (1998); *Phys. Rev. Lett.* **81**, 2610 (1998).
 - [6] T. R. Weikl and R. Lipowsky, *Langmuir* **16**, 9338 (2000).
 - [7] W. Helfrich, *Z. Naturforsch.* **28C**, 693 (1973).
 - [8] S. A. Safran, *Statistical Thermodynamics of Surfaces, Interfaces and Membranes* (Westview Press, Boulder, CO, 1994).
 - [9] R. Goetz, G. Gompper, and R. Lipowsky, *Phys. Rev. Lett.* **82**, 221 (1999); E. Lindahl and O. Edholm, *Biophys. J.* **79**, 426 (2000); S. J. Marrink and A. E. Mark, *J. Phys. Chem. B* **105**, 6122 (2001).
 - [10] R. Granek, *J. Phys. II (France)* **7**, 1761 (1997).
 - [11] M. Doi and S. F. Edwards, *The Theory of Polymer Dynamics* (Clarendon Press, Oxford, 1986).
 - [12] D. L. Ermak and J. A. McCammon, *J. Chem. Phys.* **69**, 1352 (1978).
 - [13] In previous work [3] we adopted the notation “FSBD” for an algorithm restricted to harmonic potentials based on exact solution to Eq. (2). In the present work, FSBD refers to the general algorithm specified by Eq. (4).
 - [14] M. P. Sheetz, *Semin. Hematol.* **20**, 175 (1983).
 - [15] M. Tomishige *et al.*, *J. Cell Biol.* **142**, 989 (1998).
 - [16] M. J. Saxton, *Int. J. Biochem.* **22**, 801 (1990).
 - [17] D. H. Boal and S. K. Boey, *Biophys. J.* **69**, 372 (1995).
 - [18] F. L. H. Brown *et al.*, *Biophys. J.* **78**, 2257 (2000).
 - [19] R. Podgornik and V. A. Parsegian, *Langmuir* **8**, 557 (1992).
 - [20] K. Gawrisch *et al.*, *Biophys. J.* **61**, 1213 (1992).
 - [21] D. K. Fygenson, J. F. Marko, and A. Libchaber, *Phys. Rev. Lett.* **79**, 4497 (1997).
 - [22] J.-B. Manneville *et al.*, *Phys. Rev. Lett.* **82**, 4356 (1999).
 - [23] R. Zwanzig and N. K. Ailawadi, *Phys. Rev.* **182**, 280 (1969).